

Magnetic field effect in stripe-ordered 214 ($\text{La}_{1.6-x}\text{Nd}_{0.4}\text{Sr}_x\text{CuO}_4$ and $\text{La}_{2-x}\text{Ba}_x\text{CuO}_4$) superconducting cuprates studied by resonant soft x-ray scattering

S. Blanco-Canosa,^{1,2,3,*} E. Schierle,⁴ Z. W. Li,⁵ H. Guo,⁵ T. Adachi,⁶ Y. Koike,⁷ O. Sobolev,⁸ E. Weschke,⁴ A. C. Komarek,⁵ and C. Schüller-Langeheine⁴

¹CIC nanoGUNE, 20018 Donostia-San Sebastian, Basque Country, Spain

²IKERBASQUE, Basque Foundation for Science, 48011 Bilbao, Basque Country, Spain

³Donostia International Physics Center, DIPC, 20018 Donostia-San Sebastian, Basque Country, Spain

⁴Helmholtz-Zentrum Berlin für Materialien und Energie, Albert-Einstein-Strasse 15, 12489 Berlin, Germany

⁵Max Planck Institute for Chemical Physics of Solids, Nöthnitzerstrasse 40, 01187 Dresden, Germany

⁶Department of Engineering and Applied Sciences, Sophia University 7-1 Kioi-cho, Chiyoda-ku, Tokyo 102-8554, Japan

⁷Department of Applied Physics, Tohoku University 6-6-05 Aoba, Aramaki, Aoba-ku, Sendai 980-8579, Japan

⁸Georg-August Universität, Göttingen, Institut für Physikalische Chemie, Tammannstraße 6, D-37077 Göttingen, Germany



(Received 20 January 2018; revised manuscript received 20 April 2018; published 16 May 2018)

We present a study of the charge order of 214 stripe ordered superconducting cuprates ($\text{La}_{1.6-x}\text{Nd}_{0.4}\text{Sr}_x\text{CuO}_4$ and $\text{La}_{2-x}\text{Ba}_x\text{CuO}_4$) for doping levels $0.11 \leq p \leq 0.14$ by means of resonant x-ray scattering. Up to 6 T, we find no field dependence on either the integrated intensity or the correlation length of the charge modulations, providing evidence for strong stability of charge order under applied fields. The magnetic field data support a strong pinning scenario induced by the low-temperature tetragonal distortion and static disorder, and they highlight the role of the symmetry of the lattice on the stabilization of electronic periodicities.

DOI: 10.1103/PhysRevB.97.195130

I. INTRODUCTION

The interplay between superconductivity and electronic ordering is a central theme in condensed-matter physics [1–6]. $\text{YBa}_2\text{Cu}_3\text{O}_{6+\delta}$ (YBCO) and related compounds with a minimal level of disorder exhibit a temperature and magnetic field dependence of short-ranged, weakly correlated charge periodicities [charge density wave (CDW)] for doping levels $0.08 \leq p \leq 0.15$ [7,8], which has been interpreted in terms of a competing phase with superconductivity (SC). A three-phase separation scenario (magnetic, charge, and superconductivity) has been inferred to bridge x-ray diffraction data, nuclear magnetic resonance (NMR) [9], and quantum oscillation experiments [10–12].

However, signatures of such a competing scenario are not apparent in 214 La-based cuprates: $\text{La}_{2-x}\text{Ba}_x\text{CuO}_4$ (LBCO), $(\text{La}_{1.6-x}\text{Nd}_{0.4})\text{Sr}_x\text{CuO}_4$ (LNSCO), and $(\text{La}_{1.8-x}\text{Eu}_{0.2})\text{Sr}_x\text{CuO}_4$ (LESCO). According to neutron and x-ray diffraction, charge modulations develop in 214 cuprates for doping levels $p = 0.095\text{--}0.15$ [1,13–16] showing their maximum intensity and correlation length at hole concentration $p \sim 0.125$. Moreover, connected with the stripe model in cuprates is the presence of modulation of the antiferromagnetic structure resulting in incommensurate magnetism accompanied by charge ordering (CO) [17–20].

The subtle balance between competing orders can be tuned by external perturbations like magnetic fields, pressure, or doping. In fact, the application of a magnetic field in 123-YBCO weakens SC and enhances the electronic order [6]. At

high fields, x-rays and NMR experiments in YBCO revealed a long-range anisotropic three-dimensional (3D) charge density wave along the Cu-O chain direction [9,21–23]. Elastic and inelastic neutron scattering have also shown an enhancement of the static incommensurate magnetic correlations [24].

In hole-doped $\text{La}_{2-x}\text{Ba}_x\text{CuO}_4$, 100 keV hard x-ray diffraction reported no field effect for doping levels around $p = 0.125$ [low-temperature tetragonal symmetry (LTT)]. A sizable enhancement of the charge-order peak is observed for doping levels close to the low-temperature orthorhombic (LTO) phase [25] demonstrating a competition between superconductivity and charge order in LBCO. A weak enhancement of the integrated intensity was reported for 214 $\text{La}_{1.64}\text{Eu}_{0.2}\text{Sr}_{0.16}\text{CuO}_4$, $p = 0.16$ (LESCO, $T_c = 5$ K) without affecting its correlation length [26], but no field effect has been found in electron-doped cuprates [27]. Neutron diffraction studies have indicated an enhancement of the antiferromagnetic correlations at temperatures below T_c [28–30]. In addition, transport measurements found that the superconducting transition curve shifts toward the low-temperature side in parallel with increasing field for $p = 0.11$ and 0.12 , but a *fan-shaped broadening* shift of T_c develops for dopings with orthorhombic symmetry [31–33]. It is remarkable that the strongest response of the charge order to the magnetic field has been reported for systems with orthorhombic symmetry (YBCO) [34,35], but little is known for the LTT phases [36]. Moreover, despite the approach of the theoretical models based on Coulomb interactions to describe the fermiology in the normal state of underdoped cuprates, calculations underestimate the role of the lattice potential and electron-phonon interaction [37–40].

To address these issues, we have performed a comprehensive study of the charge stripe order in LTT 214 cuprates

*s.blanco@nanogune.eu

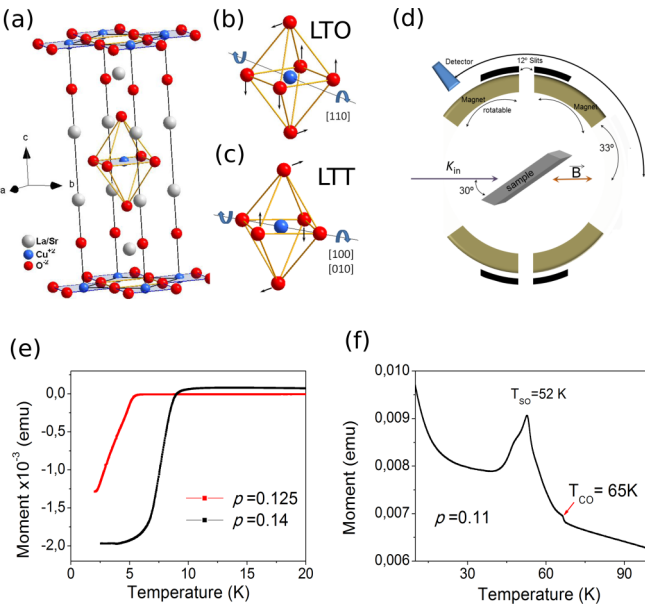


FIG. 1. (a) Crystal structure of $\text{La}_{2-x}\text{Sr}_x\text{CuO}_4$ in the high-temperature tetragonal phase (HTT, I_4/mmm). (b) Tilt directions of the CuO_6 octahedra in the low-temperature orthorhombic (LTO) and (c) low-temperature tetragonal (LTT) phase upon Nd doping. Arrows denote the tilting direction. (d) Experimental setup for the scattering measurements at the O K -edge. Selected magnetization measurements of the LNSCO and LBCO single crystals showing (e) the superconducting transition for LNSCO, $p = 0.11$ and 0.125 , and (f) magnetization curve from where the spin and charge-ordering temperatures can be seen for LNSCO, $p = 0.11$.

by means of resonant soft x-ray scattering at both Cu L - and O K -absorption edges for hole doping levels $0.11 \leq p \leq 0.14$. While hard x-ray diffraction and neutron scattering are sensitive to lattice distortions associated with electronic modulations, resonant soft x-ray scattering (REXS) allows us to study the electronic modulations at the Fermi surface. For these 214 cuprates with LTT structure, we find no magnetic field dependence of the charge modulations regarding their integrated intensities or correlation lengths. We interpret our results in the context of the more stable character of the stripe order induced by pinning to the underlying LTT octahedral tilt pattern, which shows that lattice distortions also play an important role in the three-phase competing scenario.

II. EXPERIMENTAL DETAILS

Single crystals of $(\text{La}_{1.6-x}\text{Nd}_{0.4})\text{Sr}_x\text{CuO}_4$ and $\text{La}_{2-x}\text{Ba}_x\text{CuO}_4$ (hereafter LNSCO and LBCO) measured in this work have been synthesized at the Max Planck Institute for Chemical Physics of Solids by the floating zone technique. The LBCO, $p = 0.11$ sample was also provided by Adachi and Koike and grown at Tohoku University [41]. The doping level and, therefore, T_c are controlled by chemical substitution of Sr ($p = 0.11$, 0.125 , and 0.14 ; $T_c = 7$, 5 , and 11 K, respectively) and Ba (0.11 , $T_c = 15$ K) and showing bulk superconductivity, spin, and charge order according to our SQUID magnetometry Figs. 1(e) and 1(f), and in agreement with the reports in literature [42]. Following our

field dependence of the magnetization at 4 K, the upper critical field H_{c2} is larger than 9 T. X-ray absorption (XAS) and resonant soft x-ray scattering (REXS) at zero field were performed at the UE56-PGM1 beamline, and high-field REXS up to 6 T was carried out at the UE46-PGM1 beamline at BESSY II. Samples were cleaved *in situ*. A base temperature of 4 K could be reached, thus allowing us to measure the field dependence of the charge reflections well inside the superconducting state. The in-vacuum superconducting coil of the high-field diffractometer is rotatable within the horizontal scattering plane. In the conducted experiment, the magnetic field direction was rotated by 30° with respect to the incident beam direction. At the sample angle (θ) corresponding to the maximum CO signal, this led to angles between the sample surface (CuO_2 planes) and the magnetic field of about 90° and 30° at the Cu- L and O- K resonances, respectively [see Fig. 1(d)].

The incoming beam polarization was chosen perpendicular to the scattering plane, and the background, which has been measured at high temperature, turned out to be independent of the applied magnetic field. Neutron diffraction measurements have been performed at the PUMA spectrometer at FRM II. Throughout the paper, the momentum transfer is given in reciprocal-lattice units (r.l.u.), $a^* = 2\pi/a$, $b^* = 2\pi/b$, and $c^* = 2\pi/c$, where $a = 3.79$ Å, $b = 3.79$ Å, and $c = 13.14$ Å are the lattice parameters of the HTT phase.

III. RESULTS

From a structural point of view, at low temperature $\text{La}_{2-x}\text{Ba}_x\text{CuO}_4$ transforms from orthorhombic (LTO) to tetragonal (LTT) symmetry, involving changes in the CuO_6 tilt pattern [20] [Figs. 1(a)–1(c)]. The HTT phase (space group $I4/mmm$) has the highest symmetry, without octahedral tilts. In the case of $\text{La}_{2-x}\text{Sr}_x\text{CuO}_4$, the low-temperature phase is orthorhombic and the stabilization of the LTT phase is achieved by partial substitution of Eu or Nd for La [42] with an associated rotation of the tilt axis of CuO_6 octahedra and a related change in the octahedral tilt pattern from [110] to [100] [Figs. 1(b) and 1(c)]. Büchner *et al.* [43] have defined a critical tilt angle ($\phi_c \sim 3.6^\circ$) below which the low-temperature tetragonal phase shows SC without anomalies in the transport properties. We have measured the LTT phase by following the forbidden $(001)_{\text{HTT}}$ reflection, which is observed at the O K -edge, $E = 528.5$ eV, and its temperature dependence is in agreement with the literature [14]. At lower doping levels, $p \leq 0.1$ LNSCO presents an orthorhombic symmetry.

In Fig. 2(b), the O K -edge spectra ($1s \rightarrow 2p$), which is sensitive to the valence electron ordering, shows resonances at the mobile carrier peak (MCP, 528.5 eV) and upper Hubbard band (UHB, 530.5 eV) [13]. MCP and UHB result from a $3d^9\bar{L} \rightarrow 3d^{10}$ transition of the undoped material, which is allowed due to the admixture of $3d^{10}\bar{L}$ with $3d^9$ in the ground state, where \bar{L} represents a ligand hole. When $\vec{\epsilon}$ is parallel to the ab plane, the preedge structure at 530.5 eV corresponds to O p_x and p_y states hybridized with the Cu $3d_{x^2-y^2}$ in the CuO_2 planes [44]. The preedge relative intensities depend on the hole doping due to transfer of holes from the UHB to the MCP. The charge-order peak develops a sizable intensity at

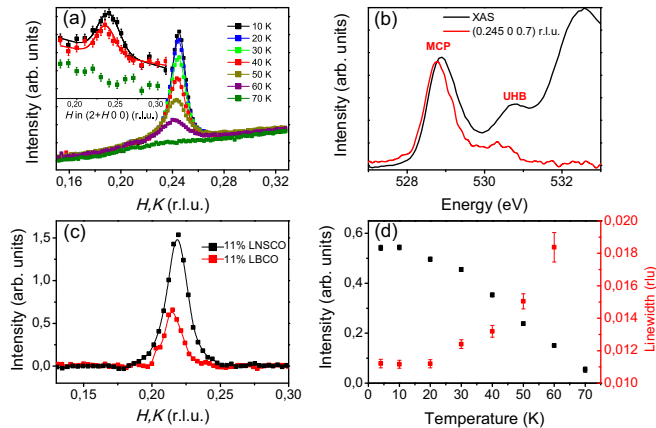


FIG. 2. (a) Temperature dependence of the charge correlations for LNSCO, $p = 0.125$ at the Cu L -edge. Inset: neutron diffraction of the CO peak at selected temperatures. Points are the experimental data, and the line is the result of the fitting. (b) XAS (black curve) showing the mobile carrier peak (MCP) and the upper Hubbard band (UHB) and charge scattering (red curve) at the O K -edge. (c) Comparison of the charge reflection of LNSCO and LBCO, $p = 0.11$ at the Cu L -edge (931 eV) at 4 K. (d) Temperature dependence of the integrated intensity and linewidth for LNSCO, $p = 0.125$.

MCP and UHB reminiscent of the “Mottness” character of the stripe order [13].

By tuning the incident photon energy to a specific x-ray absorption edge, the atomic structure factor F_n is strongly enhanced [45]. REXS experiments at the O K -edge are, therefore, directly sensitive to the valence electron states, as compared to other techniques such as neutron scattering or hard x-ray diffraction, which probe the lattice displacements induced by the modulation of the valence electron density.

The x-ray data presented here consist of H,K scans taken at the CO positions in the $(H,0,L)$ or $(0,K,L)$ planes of reciprocal space. Following synchrotron x-ray and neutron diffraction [Fig. 2(a) and inset], charge stripe order sets in below the structural transition from LTO \rightarrow LTT, and the onset of the CO and SO transitions takes place at a temperature of 70 and 50 K, respectively [46], indicating that charge rather than spin is the driving force for stripe order [47]. We found that the CO peaks are located at symmetric positions $(\delta,0,0)$ where δ is the Sr (Ba) doping, i.e., $\delta \sim p$ for $p \leq 1/8$ [see Fig. 2(a)].

The doping dependence of Q_{CO} and the charge correlations are summarized in Tables I and II, respectively. The propagation vector of the charge periodicities (δ) increases with doping following the tendency expected from the stripe model with a magnetic incommensurability δ twice that of charge order [1]. The temperature behavior of the CO follows the reports of Ref. [46] for all the doping contents studied [Fig. 2(d)].

TABLE I. Doping dependence p of the propagation vector of the stripe order peak in LNSCO and LBCO.

p	0.11_{LNSCO}	0.125_{LNSCO}	0.14_{LNSCO}	0.11_{LBCO}
$Q(\text{r.l.u.})$	0.223(3)	0.24(2)	0.254(3)	0.218(3)

TABLE II. Correlation lengths $\xi_{(a,b)}$ (\AA) for LNSCO and LBCO at the Cu L - and O K -edge (528.5 eV) at 4 K defined as $\xi_{(a,b)} = (a,b)/\pi^* \text{FWHM}$ (where a and b are the in-plane lattice parameters and FWHM is the linewidth as full width at half-maximum of the Lorentzian profile).

	$\xi_{11\% \text{LNSCO}}$	$\xi_{12.5\% \text{LNSCO}}$	$\xi_{14\% \text{LNSCO}}$	$\xi_{11\% \text{LBCO}}$
Cu L -edge	80(3)	105(2)	105(3)	95(2)
O K -edge	100(5)	130(2)	120(6)	96(3)

On the other hand, our comprehensive study of LNSCO crystals shows a similar peak intensity and linewidth for the three doping levels measured. This marks a difference as compared to LBCO, where a drop in intensity of the charge order is observed for single crystals away from $1/8$ [note that the y axis in Fig. 2(c) shows that the intensities can be compared after background subtraction and renormalization to the Cu L -edge XAS spectra]. It is known that the lock-in of the charge order at $p = 1/8$ strongly stabilizes the stripe order in LBCO and develops its maximum intensity [48]. On going away from this magic number, it appears that the CO intensity drops abruptly in LBCO but remains nearly constant for LNSCO.

We find that the linewidth of the CO peak obtained from x-ray diffraction is nearly half of that observed in our neutron scattering experiments. A much larger sample volume probed in neutron measurements ($\sim 2 \text{ cm}^3$) is generally responsible for lowering the momentum resolution compared to the x-ray case in which a mm-sized spot is used [Fig. 2(a) and inset]. Moreover, also the correlation length of LNSCO is slightly higher at MCP, which represents more itinerant electrons at the Fermi surface, than at the Cu L -edge, which picks up a substantial contribution from the lattice distortion (see Table II for values of ξ at 4 K). This suggests that the spatial extent of the ordered valence electrons is more correlated than the lattice distortion associated with the stripe order. Nevertheless, LBCO $p = 0.11$ presents a similar correlation length at both edges and reinforces the role of Nd atoms in the stabilization of the LTT tilt angle. Note that it has been shown that the superconducting transition and charge stripe order are sensitive to the degree of tilt.

Next, we present the magnetic field dependence of the stripe order for the LNSCO and LBCO samples characterized above. In cases in which SC competes with spatial electronic modulations, charge order can be significantly enhanced by the application of a c -axis magnetic field. We note here that at the Cu L -edge, the magnetic field is nearly perpendicular to the CuO_2 planes, thus reproducing the ideal scattering geometry [7,25]. Figures 3(a)–3(h) show the field-dependent spectra of the charge modulations for three different Sr contents in LNSCO and for LBCO, $p = 0.11$. No field effect can be observed at both the Cu L - and O K -edges, MCP (UHB, not shown) for either the integrated intensity or the linewidth (Fig. 4). We have performed REXS up to 6 T in LBCO, $p = 0.11$ ($T_c \sim 15$ K), observing no field effects, as in LNSCO [Figs. 3(d), 3(h), and 4]. Upon applying a magnetic field and suppression of SC, one would expect the growth of charge-ordered domains within a scenario of competing phases. We

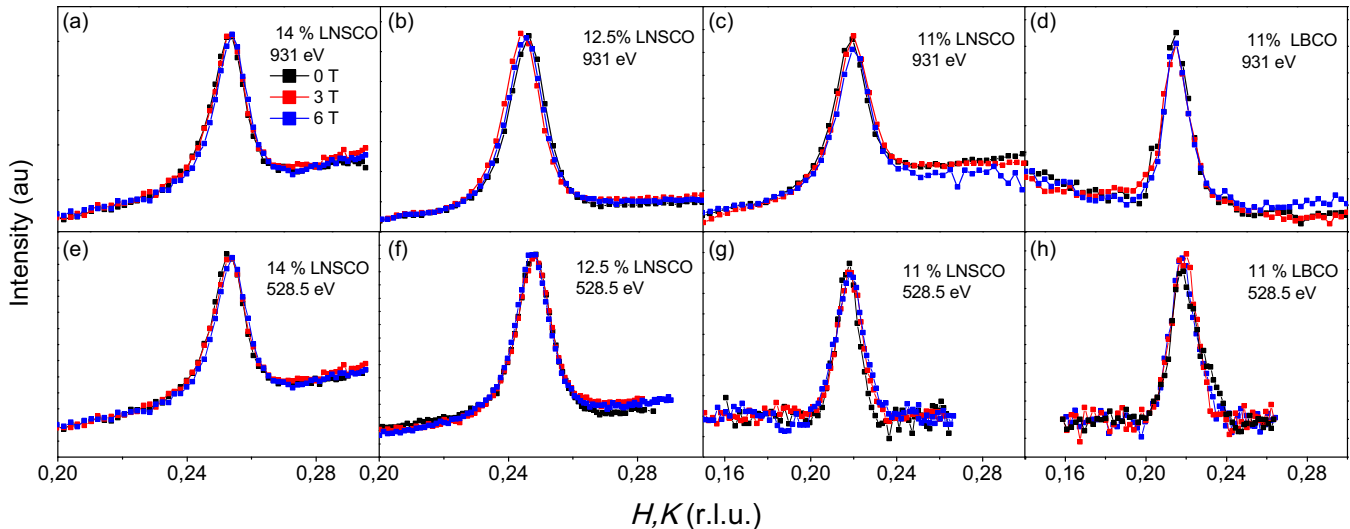


FIG. 3. (a)–(h) Magnetic field dependence of the charge stripe-order peak for LBCO, $p = 0.11$ and LNSCO, $p = 0.11, 0.125$, and 0.14 at the Cu L -edge (931.5 eV) and O K -edge (528.5 eV, mobile carrier peak) at 4 K. In (g) and (h) the background was subtracted.

point out here that correlation lengths along the c axis could not be extracted due to the limited reciprocal space available for soft x rays. Although it appears unlikely, we cannot discard a spectral weight redistribution along L related to a suppression of the superconducting phase coherence.

IV. DISCUSSION

From the results presented above, it appears that the magnetic field has no significant or visible effect on the charge stripe order either in LNSCO or LBCO single crystals at similar doping levels to those where the CDW is observed in 123 YBCO ($0.11 \leq p \leq 0.14$). We point out that one difference between 214 and 123 cuprates is the low-temperature symmetry of the lattice when CO takes place. While 123 YBCO

presents an orthorhombic symmetry and the wave vector of the CDW decreases with hole concentration, in more disordered 214 La-based cuprates the CO wave vector increases with the doping level p . A comparison between both systems also reveals a common feature: the maximum of the intensity and the correlation length is observed at $p = 0.125$, the doping where T_c is reduced.

Our comprehensive study in LNSCO samples ($T_c = 7, 5$, and 11 K) and LBCO, $p = 0.11$ and $T_c = 15$ K, has not detected any field effect at either Cu L - or O K -edges, which is in agreement with Hücker *et al.* [25]. This is in contrast with the magnetic field evolution of charge correlations in YBCO. Around the hole concentration in the CuO_2 planes, $0.08 \leq p \leq 0.15$ resonant soft x-rays detect a momentum dependence onset temperature of an incommensurate charge density modulation

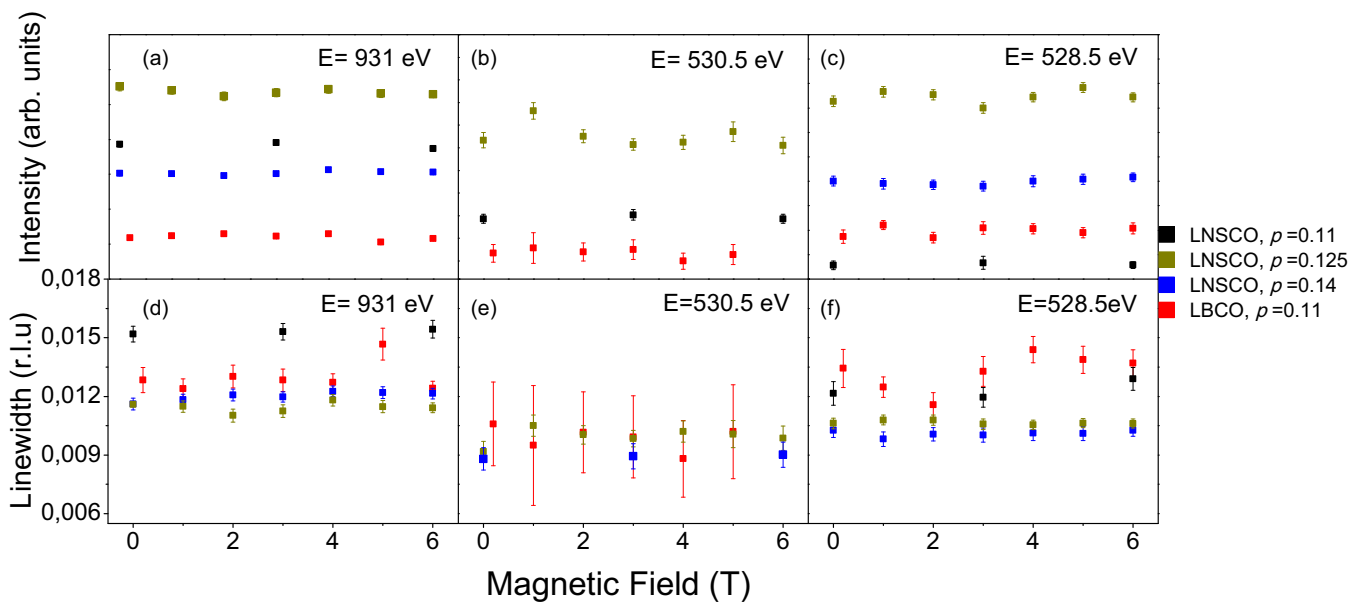


FIG. 4. Magnetic field dependence of the integrated intensity and linewidth at 4 K of the charge stripe order peak for LBCO, $p = 0.11$ and LNSCO, $p = 0.11, 0.125$, and 0.14 , respectively, at the (a,c) Cu L -edge (931.5 eV) and (b,d) O K -edge (mobile carrier peak, 528.5 eV).

in orthorhombic YBCO [7]. This order decreases below the SC transition and is enhanced if SC is weakened by a magnetic field perpendicular to the CuO₂ planes. The absence of a field effect in tetragonal LNSCO and LBCO reflects a more stable character of the charge periodicity and distinguishes 214 La-based cuprates from 123-YBCO [7]. This cannot be related to a weak competition between superconductivity and charge order, since in LBCO this competition is reflected in an enhancement of the CO under magnetic field at lower and higher doping levels where the lattice reveals an orthorhombic symmetry [25]. It is important to mention that neutron scattering measurements support a field-induced enhancement of the SDW order (or growth of the SDW volume fraction) in superconducting orthorhombic LSCO (La_{2-x}Sr_xCuO₄) and stage 4-LCO (La₂CuO₄) upon obliterating SC [28,49–51]. However, application of a 7 T field parallel to the *c* axis in LNSCO slightly increases the intensity of the magnetic peak. In addition, charge stripe order shows no change for magnetic fields up to 4 T [52], which is in agreement with our findings. Neutron data also show that the magnetic field couples to local AFM correlations of the stripe order, and the suppression of SC in vortex cores results in the nucleation of domains of stripe order without affecting its correlation length, as we see in our x-ray data. However, no observable CO intensity enhancement up to 6 T shows that there is no substantial additional nucleation of CO domains in vortex cores present in our samples. Thereby, the absence of a field effect also implies that charge-ordered regions, although stabilized by the intrinsically higher level of disorder introduced by the Nd atoms in the 214 compounds, are pinned to the tetragonal lattice distortion for octahedral tilts $\phi \leq \phi_c$ [53]. The tilt pattern in the LTT phase consists of horizontal stripes parallel to the Cu-O bonds, expecting pinning if the period of the charge stripe gets commensurate with the lattice distortion (note that for $\phi \geq \phi_c$, charge-stripe modulations are not developed). It is worth noting that da Silva *et al.* [27] also reported no field effect of the CO measured at the Cu *L*-edge in electron-doped cuprates with tetragonal symmetry for similar doping levels to those studied here.

More importantly, the data at the O *K*-edge also indicate that the electronic order at the Fermi surface remains unaltered after breaking the Cooper pairs, therefore discarding an enhancement of hole localization by the applied field. The absence of a field effect in hole- and electron-doped cuprates [27] evidences the strong stability of the stripe order in the LTT phase, presumably resulting from the electron-lattice coupling. Thereby, structural details within the 214 family of cuprates are important to understand the different behavior under a magnetic field.

V. CONCLUSION

In summary, we have presented a study of the charge stripe order in 214 La-based cuprates (La_{1.6-x}Nd_{0.4})Sr_xCuO₄ in magnetic fields at both Cu *L*- and O *K*-edge. We observe no field effect on the stripe order, indicative of a more stable character of the CO in the LTT phases than in YBCO for a similar doping level. We attribute this to the pinning to LTT structural distortion. Hence, the magnetic field effect can be observed in systems with orthorhombic symmetry, 123-YBCO and 214 La-based cuprates away from the commensurate 1/8 LTT phase, and orthorhombic La_{2-x}Sr_xCuO₄ [16,54,55]. The absence of a field effect at the O *K*-edge also indicates that the lattice potential and/or electron-phonon interaction have to be taken into account in the theoretical models in order to accurately reproduce the fermiology of stripe-ordered cuprates.

ACKNOWLEDGMENTS

M. Fujita is acknowledged for sharing additional LBCO single crystals to those chosen to measure in this work. L. H. Tjeng and P. Thalmeier are acknowledged for support and helpful discussions. S.B.-C. thanks IKERBASQUE and the Spanish Ministry of Economy, Industry and Competitiveness under the Maria de Maeztu Units of Excellence Programme-MDM-2016-0618.

-
- [1] J. M. Tranquada, B. J. Sternlieb, J. D. Axe, Y. Nakamura, and S. Uchida, *Nature (London)* **375**, 561 (1995).
 - [2] G. Ghiringhelli, M. Le Tacon, M. Minola, S. Blanco-Canosa, C. Mazzoli, N. B. Brookes, G. M. De Luca, A. Frano, D. G. Hawthorn, F. He, T. Loew, M. Moretti Sala, D. C. Peets, M. Salluzzo, E. Schierle, R. Sutarto, G. A. Sawatzky, E. Weschke, B. Keimer, and L. Braicovich, *Science* **337**, 821 (2012).
 - [3] R. Comin, A. Frano, M. M. Yee, Y. Yoshida, H. Eisaki, E. Schierle, E. Weschke, R. Sutarto, F. He, A. Soumyanarayanan, Y. He, M. Le Tacon, I. S. Elfimov, J. E. Hoffman, G. A. Sawatzky, B. Keimer, and A. Damascelli, *Science* **343**, 390 (2014).
 - [4] Eduardo H. d. Silva, P. Aynajian, A. Frano, R. Comin, E. Schierle, E. Weschke, A. Gyenis, J. Wen, J. Schneeloch, Z. Xu, S. Ono, G. Gu, M. Le Tacon, and A. Yazdani, *Science* **393**, 343 (2014).
 - [5] W. Tabis, Y. Li, M. Le Tacon, L. Braicovich, A. Kreyssig, M. Minola, G. Dellea, E. Weschke, M. J. Veit, M. Ramazanoglu, A. I. Goldman, T. Schmitt, G. Ghiringhelli, N. Barišić, M. K. Chan, C. J. Dorow, G. Yu, X. Zhao, B. Keimer, and M. Greven, *Nat. Commun.* **5**, 5875 (2014).
 - [6] J. Chang, E. Blackburn, A. T. Holmes, N. B. Christensen, J. Larsen, J. Mesot, R. Liang, D. A. Bonn, W. N. Hardy, A. Watenphul, M. v. Zimmermann, E. M. Forgan, and S. M. Hayden, *Nat. Phys.* **8**, 871 (2012).
 - [7] S. Blanco-Canosa, A. Frano, E. Schierle, J. Porras, T. Loew, M. Minola, M. Bluschke, E. Weschke, B. Keimer, and M. Le Tacon, *Phys. Rev. B* **90**, 054513 (2014).
 - [8] M. Hücker, N. B. Christensen, A. T. Holmes, E. Blackburn, E. M. Forgan, R. Liang, D. A. Bonn, W. N. Hardy, O. Gutowski, M. v. Zimmermann, S. M. Hayden, and J. Chang, *Phys. Rev. B* **90**, 054514 (2014).
 - [9] T. Wu, H. Mayaffre, S. Krämer, M. Horvatic, C. Berthier, W. N. Hardy, R. Liang, D. A. Bonn, and M. H. Julien, *Nature (London)* **477**, 191 (2011).
 - [10] N. Doiron-Leyraud, C. Proust, D. LeBoeuf, J. Levallois, J.-B. Bonnemaison, R. Liang, D. A. Bonn, W. N. Hardy, and L. Taillefer, *Nature* **447**, 565 (2007).

- [11] D. LeBoeuf, N. Doiron-Leyraud, J. Levallois, R. Daou, J.-B. Bonnemaison, N. E. Hussey, L. Balicas, B. J. Ramshaw, R. Liang, D. A. Bonn, W. N. Hardy, S. Adachi, C. Proust, and L. Taillefer, *Nature (London)* **450**, 533 (2007).
- [12] S. E. Sebastian, N. Harrison, F. F. Balakirev, M. M. Altarawneh, P. A. Goddard, R. Liang, D. A. Bonn, W. N. Hardy, and G. G. Lonzarich, *Nature (London)* **511**, 61 (2014).
- [13] P. Abbamonte, A. Rusydi, S. Smadici, G. D. Gu, G. A. Sawatzky, and D. L. Feng, *Nat. Phys.* **1**, 155 (2005).
- [14] J. Fink, V. Soltwisch, J. Geck, E. Schierle, and E. W. B. Büchner, *Phys. Rev. B* **83**, 092503 (2011).
- [15] J. Fink, E. Schierle, E. Weschke, J. Geck, D. Hawthorn, V. Soltwisch, H. Wadati, H.-H. Wu, H. A. Dürr, N. Wizent, B. Büchner, and G. A. Sawatzky, *Phys. Rev. B* **79**, 100502(R) (2009).
- [16] H.-H. Wu, M. Buchholz, C. Trabant, C. F. Chang, A. C. Komarek, F. Heigl, M. v. Zimmermann, M. Cwik, F. Nakamura, M. Braden, and C. Schüssler-Langeheine, *Nat. Commun.* **3**, 1023 (2012).
- [17] M. Fujita, H. Goka, K. Yamada, J. M. Tranquada, and L. P. Regnault, *Phys. Rev. B* **70**, 104517 (2004).
- [18] J. M. Tranquada, H. Woo, T. G. Perring, H. Goka, G. D. Gu, G. Xu, M. Fujita, and K. Yamada, *Nature (London)* **429**, 534 (2004).
- [19] E. S. Bozin, R. Zhong, K. R. Knox, G. Gu, J. P. Hill, J. M. Tranquada, and S. J. L. Billinge, *Phys. Rev. B* **91**, 054521 (2015).
- [20] M. Hücker, M. v. Zimmermann, G. D. Gu, Z. J. Xu, J. S. Wen, G. Xu, H. J. Kang, A. Zheludev, and J. M. Tranquada, *Phys. Rev. B* **83**, 104506 (2011).
- [21] S. Gerber, H. Jang, H. Nojiri, S. Matsuzawa, H. Yasumura, D. A. Bonn, R. Liang, W. N. Hardy, Z. Islam, A. Mehta, S. Song, M. Sikorski, D. Stefanescu, Y. Feng, S. A. Kivelson, T. P. Devereaux, Z.-X. Shen, C.-C. Kao, W.-S. Lee, D. Zhu, and J.-S. Lee, *Science* **350**, 949 (2015).
- [22] J. Chang, E. Blackburn, O. Ivashko, A. T. Holmes, N. B. Christensen, M. Hücker, R. Liang, D. A. Bonn, W. N. Hardy, U. Rütt, M. v. Zimmermann, E. M. Forgan, and S. M. Hayden, *Nat. Commun.* **7**, 11494 (2016).
- [23] T. Wu, H. Mayaffre, S. Krämer, M. Horvatic, C. Berthier, W. N. Hardy, R. Liang, D. A. Bonn, and M. H. Julien, *Nat. Commun.* **6**, 6438 (2015).
- [24] D. Haug, V. Hinkov, A. Suchaneck, D. S. Inosov, N. B. Christensen, Ch. Niedermayer, P. Bourges, Y. Sidis, J. T. Park, A. Ivanov, C. T. Lin, J. Mesot, and B. Keimer, *Phys. Rev. Lett.* **103**, 017001 (2009).
- [25] M. Hücker, M. v. Zimmermann, Z. J. Xu, J. S. Wen, G. D. Gu, and J. M. Tranquada, *Phys. Rev. B* **87**, 014501 (2013).
- [26] M. Zwiebler, E. Schierle, E. Weschke, B. Büchner, A. Recolevski, P. Ribeiro, J. Geck, and J. Fink, *Phys. Rev. B* **94**, 165157 (2016).
- [27] E. H. da Silva Neto, B. Yu, M. Minola, R. Sutarto, E. Schierle, F. Boschini, M. Zonno, M. Bluschke, J. Higgins, Y. Li, G. Yu, E. Weschke, F. He, M. Le Tacon, R. L. Greene, M. Greven, G. A. Sawatzky, B. Keimer, and A. Damascelli, *Sci. Adv.* **2**, e1600782 (2016).
- [28] B. Lake, H. M. Ronnow, N. B. Christensen, G. Aepli, K. Lefmann, D. F. McMorrow, P. Vorderwisch, P. Smeibidl, N. Mangkorntong, T. Sasagawa, M. Nohara, H. Takagi, and T. E. Mason, *Nature (London)* **415**, 299 (2002).
- [29] J. Chang, Ch. Niedermayer, R. Gilardi, N. B. Christensen, H. M. Ronnow, D. F. McMorrow, M. Ay, J. Stahn, O. Sobolev, A. Hiess, S. Pailhes, C. Baines, N. Momono, M. Oda, M. Ido, and J. Mesot, *Phys. Rev. B* **78**, 104525 (2008).
- [30] J. Wen, Z. Xu, G. Xu, J. M. Tranquada, G. Gu, S. Chang, and H. J. Kang, *Phys. Rev. B* **78**, 212506 (2008).
- [31] T. Adachi, N. Kitajima, T. Manabe, Y. Koike, K. Kudo, T. Sasaki, and N. Kobayashi, *Phys. Rev. B* **71**, 104516 (2005).
- [32] Y. Koike and T. Adachi, *Physica C* **481**, 115 (2012).
- [33] K. Kudo, M. Yamazaki, T. Kawamata, T. Adachi, T. Noji, Y. Koike, T. Nishizaki, and N. Kobayashi, *Phys. Rev. B* **70**, 014503 (2004).
- [34] S. Blanco-Canosa, A. Frano, T. Loew, Y. Lu, J. Porras, G. Ghiringhelli, M. Minola, C. Mazzoli, L. Braicovich, E. Schierle, E. Weschke, M. Le Tacon, and B. Keimer, *Phys. Rev. Lett.* **110**, 187001 (2013).
- [35] E. Blackburn, J. Chang, M. Hücker, A. T. Holmes, N. B. Christensen, R. Liang, D. A. Bonn, W. N. Hardy, U. Rütt, O. Gutowski, M. v. Zimmermann, E. M. Forgan, and S. M. Hayden, *Phys. Rev. Lett.* **110**, 137004 (2013).
- [36] M. Fujita, M. Matsuda, H. Goka, T. Adachi, Y. Koike, and K. Yamada, *J. Phys. Conf. Ser.* **51**, 510 (2006).
- [37] A. Himeda, T. Kato, and M. Ogata, *Phys. Rev. Lett.* **88**, 117001 (2002).
- [38] C. S. Hellberg and E. Manousakis, *Phys. Rev. Lett.* **83**, 132 (1999).
- [39] T. Tohyama and S. Maekawa, *Phys. Rev. B* **49**, 3596 (1994).
- [40] C. Castellani, C. Di Castro, and M. Grilli, *Phys. Rev. Lett.* **75**, 4650 (1995).
- [41] T. Adachi, T. Noji, and Y. Koike, *Phys. Rev. B* **64**, 144524 (2001).
- [42] J. M. Tranquada, J. D. Axe, N. Ichikawa, A. R. Moodenbaugh, Y. Nakamura, and S. Uchida, *Phys. Rev. Lett.* **78**, 338 (1997).
- [43] B. Büchner, M. Breuer, A. Freimuth, and A. P. Kampf, *Phys. Rev. Lett.* **73**, 1841 (1994).
- [44] C. T. Chen, L. H. Tjeng, J. Kwo, H. L. Kao, P. Rudolf, F. Sette, and R. M. Fleming, *Phys. Rev. Lett.* **68**, 2543 (1992).
- [45] J. Fink, E. Schierle, E. Weschke, and J. Geck, *Rep. Prog. Phys.* **76**, 056502 (2013).
- [46] J. M. Tranquada, J. D. Axe, N. Ichikawa, Y. Nakamura, S. Uchida, and B. Nachumi, *Phys. Rev. B* **54**, 7489 (1996).
- [47] O. Zachar, S. A. Kivelson, and V. J. Emery, *Phys. Rev. B* **57**, 1422 (1998).
- [48] S. B. Wilkins, M. P. M. Dean, J. Fink, M. Hücker, J. Geck, V. Soltwisch, E. Schierle, E. Weschke, G. Gu, S. Uchida, N. Ichikawa, J. Tranquada, and J. P. Hill, *Phys. Rev. B* **84**, 195101 (2011).
- [49] B. Khaykovich, Y. S. Lee, R. Erwin, S.-H. Lee, S. Wakimoto, K. J. Thomas, M. A. Kastner, and R. J. Birgeneau, *Phys. Rev. B* **66**, 014528 (2002).
- [50] B. Khaykovich, R. J. Birgeneau, F. C. Chou, R. W. Erwin, M. A. Kastner, S.-H. Lee, Y. S. Lee, P. Smeibidl, P. Vorderwisch, and S. Wakimoto, *Phys. Rev. B* **67**, 054501 (2003).
- [51] S. Katano, M. Sato, K. Yamada, T. Suzuki, and T. Fukase, *Phys. Rev. B* **62**, R14677 (2000).
- [52] S. Wakimoto, R. J. Birgeneau, Y. Fujimaki, N. Ichikawa, T. Kasuga, Y. J. Kim, K. M. Kojima, S.-H. Lee, H. Niko, J. M. Tranquada, S. Uchida, and M. v. Zimmermann, *Phys. Rev. B* **67**, 184419 (2003).
- [53] D. Axe and M. K. Crawford, *J. Low Temp. Phys.* **95**, 271 (1994).

- [54] V. Thampy, M. P. M. Dean, N. B. Christensen, L. Steinke, Z. Islam, M. Oda, M. Ido, N. Momono, S. B. Wilkins, and J. P. Hill, *Phys. Rev. B* **90**, 100510(R) (2014).
- [55] N. B. Christensen, J. Chang, J. Larsen, M. Fujita, M. Oda, M. Ido, N. Momono, E. M. Forgan, A. T. Holmes, J. Mesot, M. Huecker, and M. v. Zimmermann, [arXiv:1404.3192](https://arxiv.org/abs/1404.3192).